DOI: 10.6060/ivkkt.20246712.7152

УДК: 544.3.032.2:[666.762.11+666.762.64]

РЕАКЦИОННАЯ СПОСОБНОСТЬ АЛЮМООКСИДНЫХ ПРЕКУРСОРОВ ДЛЯ ТВЕРДОФАЗНОГО ОБРАЗОВАНИЯ ШПИНЕЛИ $MgAl_2O_4$

Н.В. Филатова, Н.Ф. Косенко, А.С. Артюшин, М.С. Малоиван, И.И. Зонина, А.С. Власенков

Наталья Владимировна Филатова (ORCID 0000-0001-7552-3496)*, Надежда Федоровна Косенко (ORCID 0000-0001-8806-7530), Артем Сергеевич Артюшин, Мария Сергеевна Малоиван, Ирина Игоревна Зонина, Алексей Станиславович Власенков

Ивановский государственный химико-технологический университет, кафедра технологии керамики и электрохимических производств, пр. Шереметевский, 7, Иваново, Российская Федерация, 153000
E-mail: zyanata@mail.ru*, nfkosenko@gmail.com, artyushin_as@mail.ru, maloivan2017@mail.ru, zoninairina@gmail.com, vasanpolka@mail.ru

Сопоставлена реакционная способность различных алюмооксидных прекурсоров в реакции образования магнезиальной шпинели: промышленного производства (корундового порошка КП (KP), глиноземов: металлургического ГК (GK), неметаллургического Г-00 (G-00), реактивного РГ (RG)) и продукта горения ксерогеля из нитрата алюминия с лимонной кислотой в условиях механоактивирующей обработки и без нее. Проанализированы ИК-спектры корунда и периклаза после механической обработки разного типа (ударно-истирающей в планетарной мельнице, истирания в шаро-кольцевой мельнице). Установлено, что кратковременное воздействие не только активировало компоненты, но и способствовало разрушению адсорбционных соединений на стадии подготовки. Проанализировано влияние механоактивации реагентов на выход шпинели. Установлено, что алюмооксидный продукт горения ксерогеля без отжига являлся рентгеноаморфным, что предполагало его высокую химическую активность. При его использовании обнаружено более полное связывание исходных реагентов в продукт по сравнению со смесью периклаза и корунда. Даже в отсутствие механоактивации компонентов удавалось достичь высокого выхода шпинели (до 80%). Полученные значения эффективных констант скорости реакции свидетельствуют о большей результативности механической обработки, включающей в себя ударную компоненту, при совместной активации периклаза и корунда/глинозема. Совместная обработка реагентов в планетарной мельнице (ПМ) позволила увеличить скорость реакции в 5-6,5 раз, тогда как истирание в шаро-кольцевой мельнице – всего в 1,7 раза. Предварительная обработка одного из компонентов исходной смеси в ПМ наиболее целесообразна для периклаза, поскольку она дала возможность ускорить реакцию в ~ 5 раз, а также наиболее выгодна энергетически и технологически из-за обработки только одного компонента пониженной твердости. Применение в синтезе шпинели продукта горения ксерогеля весьма эффективно, т.к. ускорило процесс в ~4 раза даже без предварительной активации механическим способом.

Ключевые слова: шпинель, $MgAl_2O_4$, твердофазный синтез, кинетика, механоактивация, корунд, глинозем, периклаз, механоактивация, ИК-спектры, продукт горения ксерогеля

REACTIVITY OF ALUMINUM OXIDE PRECURSORS FOR SOLID-PHASE FORMATION OF $MgAl_2O_4$ SPINEL

N.V. Filatova, N.F. Kosenko, A.S. Artyushin, M.S. Maloivan, I.I. Zonina, A.S. Vlasenkov

Natalya V. Filatova(ORCID 0000-0001-7552-3496)*, Nadezhda F. Kosenko (ORCID 0000-0001-8806-7530), Artyom S. Artyushin, Maria S. Maloivan, Irina I. Zonina, Aleksey S. Vlasenkov

Department of Ceramics Technology and Electrochemical Production, Ivanovo State University of Chemistry and Technology, Sheremetevskiy ave., 7, Ivanovo, 153000, Russia
E-mail: zyanata@mail.ru *, nfkosenko@gmail.com, artyushin_as@mail.ru, maloivan2017@mail.ru, zoninairina@gmail.com, vasanpolka@mail.ru

The reactivity of various alumina precursors in the reaction of magnesia spinel formation is compared: industrial powders (corundum powder KP, alumina: metallurgical GC, non-metallurgical G-00, reactive RG) and the xerogel combustion product from aluminum nitrate with citric acid under conditions of mechanical activating treatment and without it. The infrared spectra of corundum and periclase after mechanical treatment of various types (impact-abrasion in a planetary mill, abrasion in a ball-ring mill) were analyzed. It has been found that short-term action not only activated the components, but also contributed to the destruction of adsorption compounds at the preparation stage. The effect of mechanical activation of reagents on spinel yield was analyzed. It has been established that the alumina xerogel combustion product without annealing was X-ray amorphous, which suggested its high chemical activity. When using it, a more complete binding of initial reagents into the product was found compared to a mixture of periclase and corundum. Even in the absence of mechanical activation of the components, it was possible to achieve a high spinel yield (up to 80%). The obtained values of the effective reaction rate constants indicated a greater efficiency of mechanical treatment, including an impact component, with the combined activation of periclase and corundum/alumina. Co-treatment of reagents in a planetary mill (PM) made it possible to increase the reaction rate by 6-6.5 times, while abrasion in a ball-ring mill was only 1.7 times. Pretreatment of one component of the initial mix in PM was the most expedient for periclase, since it allowed to speed up the reaction by ~ 5 times, and is also the most profitable energetically and technologically due to the treatment of only one component of reduced hardness. The use of xerogel combustion product in the spinel synthesis was very effective, because it accelerated the process by ~4 times even without preliminary activation by mechanical means.

Keywords: spinel, $MgAl_2O_4$, solid-state synthesis, kinetics, mechanical activation, corundum, alumina, periclase, mechanical activation, infrared spectra, xerogel combustion product

Для цитирования:
Филатова Н.В., Косенко Н.Ф., Артюшин А.С., Малоиван М.С., Зонина И.И., Власенков А.С. Реакционная способность алюмооксидных прекурсоров для твердофазного образования шпинели $MgAl_2O_4$. *Изв. вузов. Химия и хим. технология*. 2024. Т. 67. Вып. 12. С. 15–24. DOI: 10.6060/ivkkt.20246712.7152.

For citation:
Filatova N.V., Kosenko N.F., Artyushin A.S., Maloivan M.S., Zonina I.I., Vlasenkov A.S. Reactivity of aluminum oxide precursors for solid-phase formation of $MgAl_2O_4$ spinel. *ChemChemTech [Izv. Vyssh. Uchebn. Zaved. Khim. Khim. Tekhnol.]*. 2024. V. 67. N 12. P. 15–24. DOI: 10.6060/ivkkt.20246712.7152.

INTRODUCTION

In recent decades, spinels have become widespread in various areas of material production, including ceramics, refractory products, catalysts, pigments, a variety of composites, and more.

The magnesia spinel (MS) $MgAl_2O_4$ is the most well-known of this group, having the general formula $M^{II}M^{III}_2O_4$, where M^{II} and M^{III} are divalent and trivalent metal cations, respectively. MS has a unique set of physicochemical and operational characteristics: high melting point (~2135 °C), significant density (3.584 g/cm^3) [1], high hardness (8 on the Mohs scale), mechanical strength [2, 3], which remains significant at high temperatures, low dielectric losses, good heat resistance, chemical and radiation resistance, low coefficient of thermal expansion, excellent resistance to acids and alkalis [4], etc. It should also be noted that, unlike many other refractory systems, the eutectics in the MgO-Al_2O_3 system are also high-temperature (> 1900 °C).

MS is now widely used for the production of a variety of ceramic and refractory products [5-11]. $MgAl_2O_4$ spinel is incorporated in refractories to increase the high temperature durability in high demanding applications such as purging plugs or impact pads [12]. The MS use is also based on its optical properties [3, 13-16] and photoactivity [17, 18]. Luminescent materials [19], sensors [20], catalysts [21, 22] are made from MS. Spinel sol has been proposed as a binder in alumina refractories (castable) [23] and silicon carbide ceramics [24].

In this regard, it is understandable that interest in this compound has not decreased for more than half a century. The ever-increasing demand for this product stimulates the development of new and improvement of known methods for its production, such as ceramic synthesis [25], coprecipitation [26-29], sol-gel method [30-35], decomposition of double hydroxides [36], combustion [37-44], high-temperature self-propagating synthesis [45, 46], etc.

In industry, spinel is produced by solid-phase sintering or melting of mixtures of industrial powders [8,25, 47].

Corundum (α-Al_2O_3) and periclase (MgO) are known to be thermodynamically and kinetically stable, and therefore have low reactivity. In order to intensify the interaction of oxides, corundum and periclase are replaced by more active forms [48-52], and microwave [53-55] or mechanical [25, 55-59] treatment is used. Mechanical activation is a very common method of increasing the reactivity of various substances and materials, including for the spinel production. Most often, mechanochemical reactions are carried out in high-energy planetary impact-abrasion mills. The abrasion effect on solid-phase processes remains poorly understood [25, 60, 61].

The aim of this study was to compare the reactivity of alumina precursors by studying the kinetics of $MgAl_2O_4$ solid-phase synthesis after treatment of initial oxides in activators. For the first time, alumina powder obtained by xerogel combustion was taken as one of the sources of Al_2O_3.

MATERIALS AND EXPERIMENTS

Industrial powders of sintered periclase with a 5-15 μm fraction content of at least 70%, fused corundum (at least 80% of particles with a size of 20-25 μm, specific surface area according to BET 0.45 m^2/g), metallurgical alumina grade G-00 (GOST 30558-98), non-metallurgical alumina grade GK (GOST 30559-98), reactive alumina (RG; TU 6-09-3916-75) with a specific surface area of 0.50; 0.71; 105 m^2/g, respectively, were used.

To obtain alumina powder by combustion, aluminium nitrate crystal hydrate $Al(NO_3)_3 \cdot 9H_2O$ was taken as an oxidizer and citric acid $C_6H_8O_7$ as a fuel in a stoichiometric ratio according to the following reaction equation:

$$6[Al(NO_3)_3 \cdot 9H_2O] + 5C_6H_8O_7 \rightarrow$$
$$\rightarrow 3Al_2O_3 + 30CO_2\uparrow + 74H_2O + 9N_2\uparrow$$

Concentrated solutions of nitrate and acid were mixed to form a transparent gel, from which a xerogel was obtained by drying at 70-90 °C. The latter was ignited by heating on an electric stove at a temperature of 200-300 °C. The combustion product was pounded in a mortar; part of it was annealed at 500 °C.

Mechanical processing was carried out in two types of laboratory mills: in a ball-ring mill (BRM), operating on the principle of abrasion; in the AGO-2 planetary mill (PM), the action of which includes an impact component.

IR spectra of samples were obtained on the device "Avatar 360-FT-IR" (company "Nicolet") in the region of 500-4000 cm^{-1}.

The specific surface area of powders was determined on the Sorby M device using nitrogen adsorption-desorption data and the BET method.

Scanning electron microscopy (Vega 3 SBH) was used to describe the morphology of the crystals.

Charges were prepared by simple mixing the components; mixing oxides, one of which has been pre-treated in a mill; co-processing of components in a mill. The initial substances were taken in quantities corresponding to their stoichiometric ratio in spinel. Tablets were pressed (200 MPa) from the reaction mixtures using a 5% solution of polyacrylic acid. The samples were then fired at 1300 °C.

The yield of $MgAl_2O_4$ was determined by quantitative X-ray phase analysis (d = 0.143 and 0.105 nm) using the DRON-6 diffractometer [62]. For control, thermogravimetric analysis was performed (by weighing the insoluble residue in concentrated hydrochloric acid).

RESULTS

It is known that industrial oxide objects often contain some adsorbed water, so at high temperatures a partial change in the periclase component (MgO) due to hydration is possible. The presence of hydrate water, OH- and CO_3-groups can be conveniently monitored using IR spectroscopy. The IR spectra of spinel precursors, namely periclase and corundum after mechanical treatment, were analyzed (Fig. 1).

The initial fused corundum powder KP (curves 1 in Fig. 1, a, b) contains OH groups (valence oscillations of isolated OH^- groups at ~3700 cm^{-1}) and CO_3^{2-}-groups (valence group oscillations in the region of ~1630 and 1420-1480 cm^{-1}), and the carbonate groups are chemosorbed in positions that are energetically unequivalent, which is confirmed by splitting a wide single band into a clearly distinguishable doublet of sharp peaks of 1420 and 1480 cm^{-1}. There is a small amount of adsorbed water (a wide band of 3300-3600 cm^{-1} – valence fluctuations of the OH-groups of molecular water). In the short-wave region, there is a strong absorption in the region of 760, 750, 670, 680-500, 530, 400 cm^{-1}, characteristic of AlO_6 octahedra.

Periclase (curves 2 in Fig. 1 a, b) is characterized by the absence of peaks for OH-groups, there are very faint bands of CO_3^{2-}-groups; there is adsorbed water. In the short-wavelength region, moderate absorption is in the region of 450-750 cm^{-1}, corresponding to a highly extended band with a maximum absorption of ~ 580-590 cm^{-1} (valence oscillations of MgO_6 groups).

After treatment in the planetary mill, changes in the corundum spectrum (Fig. 1 a, curve 3) indicate the destruction of all compounds formed as a result of

chemisorption. A strong amorphization becomes apparent, confirmed by an absorption decrease in the entire range of wave numbers and by the absence of pronounced absorption bands. Under the same conditions, initially inactive periclase is activated, which is accompanied by the addition of OH^- and CO_3^{2-} due to chemosorption (Fig. 1 a, curve 4).

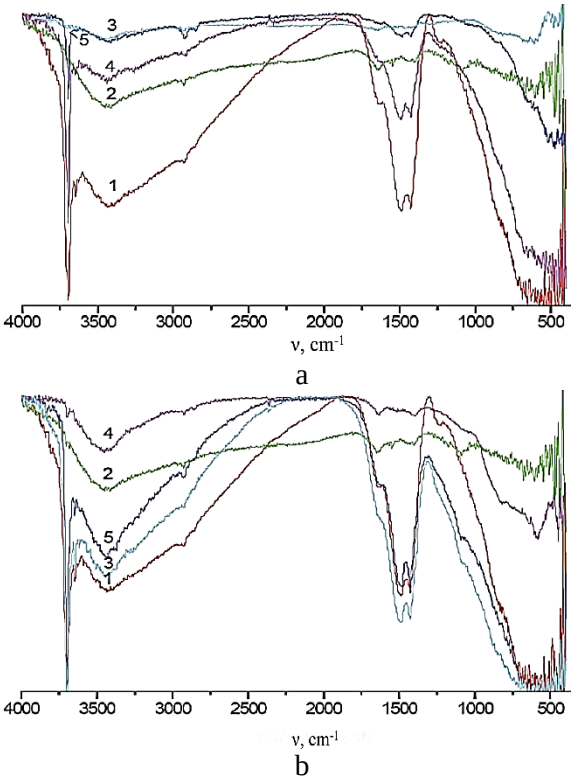

Fig. 1. IR spectra of initial (1,2) and processed (3,4,5) oxides in planetary (a) and ball-ring mill (b): 1,3 – corundum; 2,4 – periclase; 5 – corundum + periclase. Machining time, min: a – 20; b – 5

Рис. 1. ИК спектры исходных (1,2) и обработанных (3,4,5) в планетарной (а) и шаро-кольцевой мельнице (b) оксидов: 1,3 – корунд; 2,4 – периклаз; 5 – корунд + периклаз. Время механической обработки, мин: a – 20; b – 5

Abrasive treatment of corundum in air leads to a slight increase in the content of OH^- and CO_3^{2-} (Fig. 1 b, curve 3). An increase in absorption in the region of 750-900 cm^{-1} may indicate the appearance of some aluminum in the tetrahedral coordination (AlO_4). As a result of similar treatment of periclase, a noticeable change in the nature of absorption in the short-wavelength region is observed (Fig. 1 b, curve 4): the diffuse band corresponding to the valence fluctuations of the Mg-O bonds turns into a clear line with a maximum of ~ 600 cm^{-1}, which may apparently indicate some ordering of the structure.

The IR spectra of oxide mixtures after treatment are intermediate (Fig. 1 a, b, curves 5). No new absorption bands corresponding to the appearance of the spinel phase were detected. In this way, the short pre-machining of the initial components not only activates them, but also contributes to the destruction of the adsorption compounds already in the preparation phase.

X-ray phase analysis of the xerogel combustion product (Fig. 2) indicates its high X-ray amorphousness, and therefore high chemical activity.

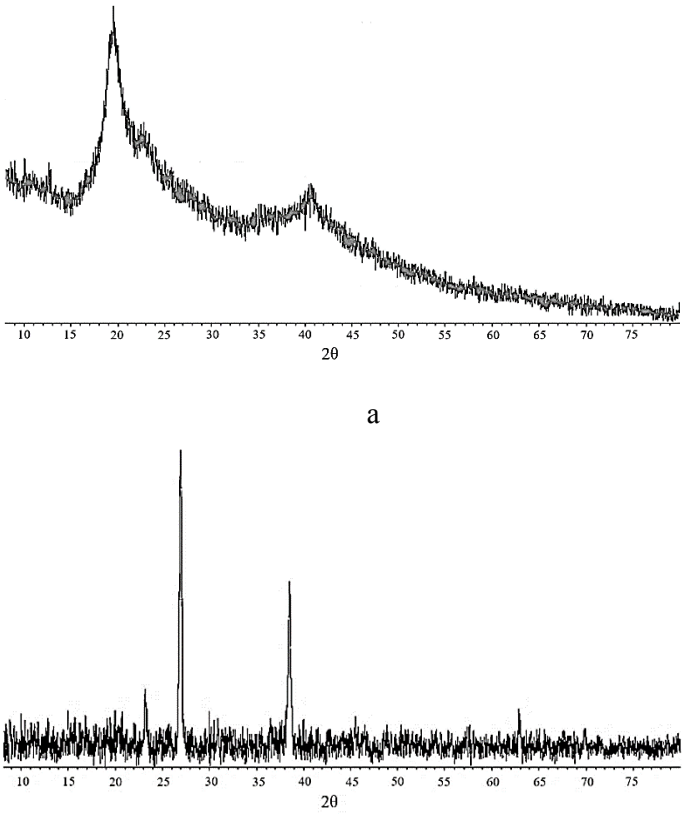

Fig. 2. XRD spectra of the xerogel combustion product from aluminum nitrate and citric acid at the ratio of the initial components 1:1 (a) and 1:1.25 (b) without annealing

Рис. 2. Дифрактограммы продукта горения ксерогеля из нитрата алюминия и лимонной кислоты при соотношении исходных компонентов 1:1 (а) и 1:1,25 (b) без отжига

When corundum was replaced by the xerogel combustion product for the spinel formation reaction, the relative content of the initial oxides, especially Al_2O_3, decreased (Fig. 3), indicating a more complete binding of the reactants.

To determine the rate constants of the spinel formation reaction, the yield of $MgAl_2O_4$ during the roasting process at 1300 °C was determined (Fig. 4). The designations of the series of experiments are given in Table 1.

Simple mixing of the components resulted in a relatively small amount of product (up to ~ 40%,

Fig. 4, curve 1). If one of the reagents is pre-treated mechanically (Fig. 4, curves 2-3), the product yield is significantly increased (up to 60-80%) due to the solid phase activation by increasing the structure defectiveness. The greater influence of periclase processing compared to corundum was explained earlier [25] by the peculiarities of the periclase crystal lattice of the halite type, which has many sliding planes, in which dislocations are more easily formed. Co-activation (Fig. 4, curve 4) leads to the maximum result, since it contributes to a significant increase in the reactants contact surface. The efficiency of the ball-ring mill is noticeably lower (Fig. 4, curve 5) due to its lower energy intensity.

If corundum powder KP is replaced by another industrial source of alumina (GK, G-00), the spinel yield remains almost the same (Fig. 4, curves 6, 7); only for reactive alumina the synthesis productivity increase slightly (Fig. 4, curve 8). This can be attributed to the fact that the specific surface area of the initial powders KP, GC and G-00 differs slightly: 0.45; 0,50; 0.71 m^2/g, respectively. Their phase composition is represented by high-temperature corundum α-Al_2O_3 (Fig. 5 a-c).

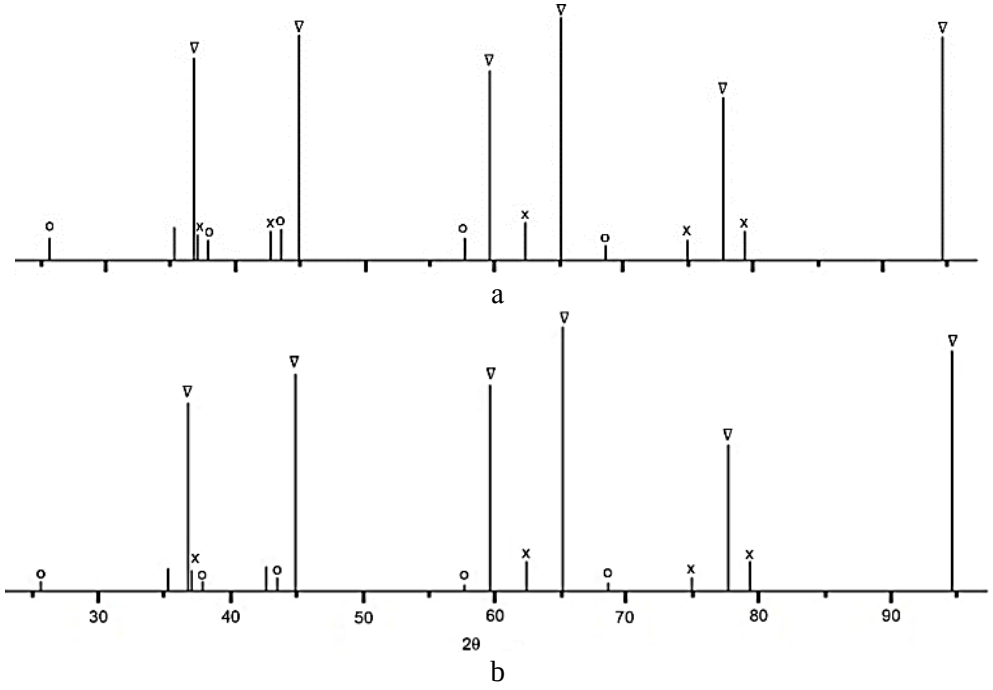

Fig. 3. Bar diagrams for machined and fired (1300 °C) mixture of periclase and corundum (a); for the fired mixture of periclase and the combustion product of aluminium nitrate with citric acid (1:1) without annealing (b). Designations: o – α-Al_2O_3; x – MgO; Ñ – $MgAl_2O_4$ Обозначения: o – α-Al_2O_3; x – MgO; ∇ – $MgAl_2O_4$

Рис. 3. Штрих-диаграммы для механически обработанной и обожженной (1300 °C) смеси периклаза и корунда (a); для обожженной смеси периклаза и продукта горения нитрата алюминия с лимонной кислотой (1:1) без отжига (b). Обозначения: o – α-Al_2O_3; x – MgO; Ñ – $MgAl_2O_4$

Table 1

Designations of a series of experiments to study the kinetics of spinel formation

***Таблица 1.* Обозначения серии экспериментов по изучению кинетики образования шпинели**

№	Method for preparing reaction mixture of initial components	Обозначение
1	A mixture made by a simple mixture of periclase and corundum	P+C
2	Mixture of periclase and corundum treated in PM	P+C(PM)
3	Mixture of PM-treated periclase and corundum	P(PM)+C
4	Mixture of periclase and corundum treated in PM	(P+C)(PM)
5	Mixture of periclase and corundum processed in BRM	(P+C)(BRM)
6	Mixture of periclase and alumina HA processed in PM	(P+GK)(PM)
7	Mixture of periclase and alumina G-00 treated in PM	(P+G-00)(PM)
8	Mixture of periclase and reactive alumina treated in PM	(P+RG)(PM)
9	Mixture of xerogel combustion product and periclase	XCP+P

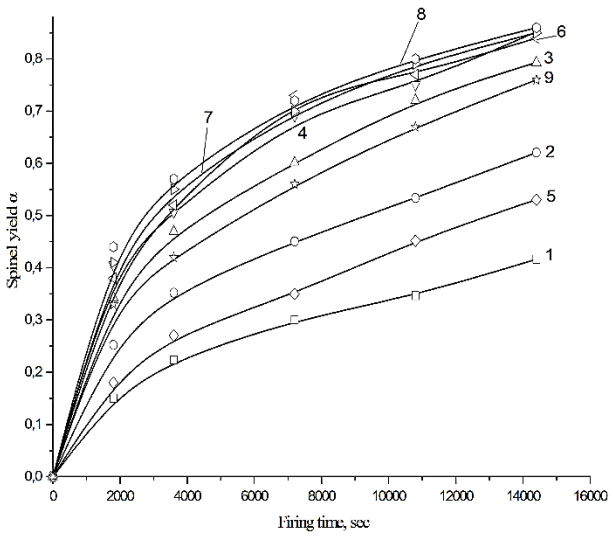

Fig. 4. Spinel yield from mixtures: P+C (1); P+C(PM) (2); P(PM)+C (3); (P+C)(PM) (4); (P+C)(BRM) (5); (P+GK)(PM) (6); (P+G-00)(PM) (7); (P+RG)(PM) (8); XCP+P (9). Firing temperature is 1300 °C

Рис. 4. Выход шпинели из смесей: П+К (1); П+К(ПМ) (2); П(ПМ)+К (3); (П+К)(ПМ) (4); (П+К)(ШКМ) (5); (П+ГК)(ПМ) (6); (П+Г00)(ПМ) (7); (П+РГ)(ПМ) (8); ПГК+П (9). Температура обжига 1300 °C

Reactive alumina is represented by a mixture of transition forms of alumina partially superimposed on each other (Fig. 5 d). They are more reactive, in addition, its specific surface area is significantly higher, which is also confirmed by microphotographs (Fig. 6 d-e). All this leads to a certain increase in the $MgAl_2O_4$ yield (Fig. 4, curve 8).

Of interest is curve 9 in Fig. 4, relating to the use of the xerogel combustion product from aluminium nitrate and citric acid as a source of Al_2O_3. Even in the absence of mechanical activation of the mixture components, it is possible to achieve a high spinel yield (up to 80%). Apparently, the formation of alumina under the conditions of the release of a huge volume of gaseous products (10 moles of CO_2, 24.6 moles of H_2O, 3 moles of N_2 per 1 mol of Al_2O_3) contributes to the breaking of chemical bonds and, as a result, leads to the absence of a well-formed crystal lattice of alumina, which increases the reactivity of this component.

To calculate the effective velocity constants, the Ginstling-Brownstein equation was used, which had previously [25] shown to be suitable for processing similar data:

$$1 - \frac{2}{3}\alpha - (1-\alpha)^{\frac{2}{3}} = K\tau, \qquad (1)$$

where α is the spinel yield (degree of transformation), ≤ 1; K is the effective reaction rate constant, sec^{-1}; τ – time, sec.

In the coordinates of this equation, dependencies with a confidence coefficient of the linear approximation R^2 of at least 0.95 were obtained (Fig. 7). Their inclination tangent yielded effective reaction rate constants (Table 2).

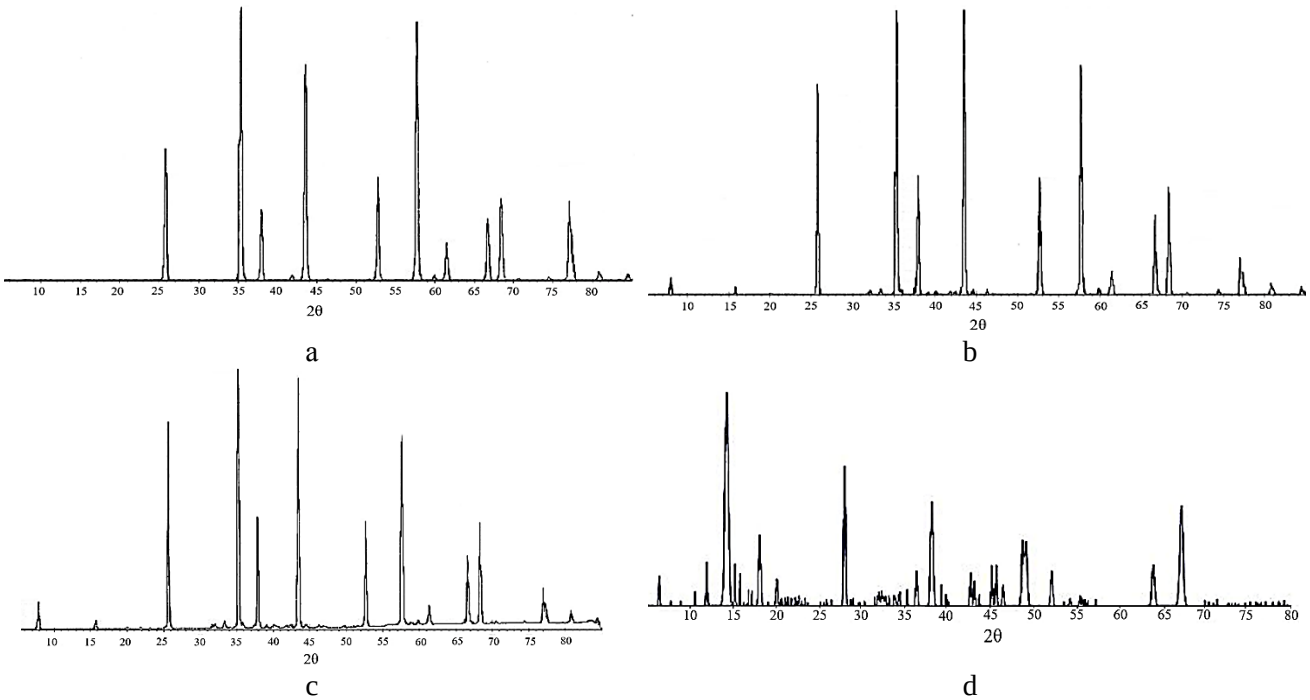

Fig. 5. XRD spectra of KP (a), GC (b), G-00 (c), RG (d)

Рис. 5. Дифрактограммы КП (a), ГК (b), Г-00 (c), РГ (d)

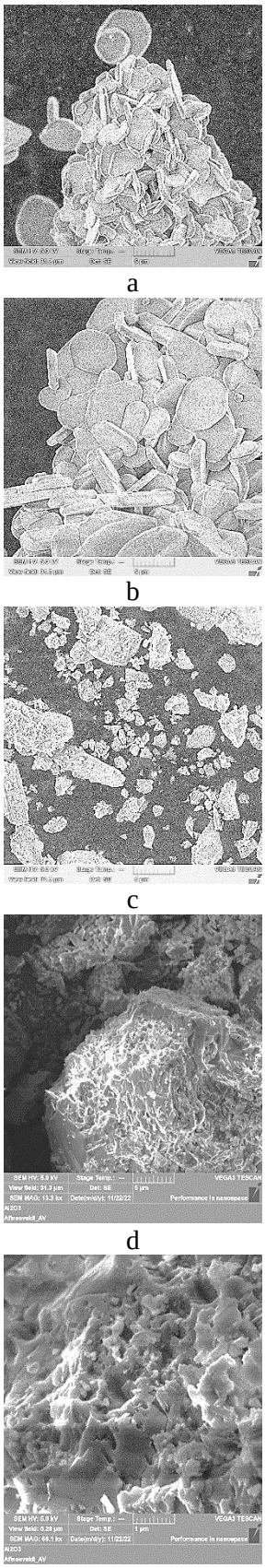

a b c d e

Fig. 6. SEM photos of KP (a), GC (b), G-00 (c), RG (d, e)
Рис. 6. СЭМ-фотографии КП (a), ГК (b), Г-00 (c), РГ (d, e)

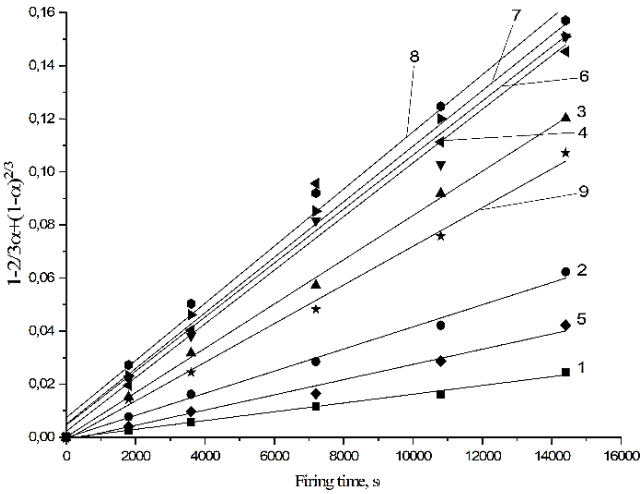

Fig. 7. Dependencies in coordinates of the Ginstling-Brownstein equation for mixtures: P+C (1); P+C(PM) (2); P(PM)+C (3); (P+C)(PM) (4); (P+C)(BRM) (5); (P+GK)(PM) (6); (P+G-00)(PM) (7); (P+RG)(PM) (8); XCP+P (9). Firing temperature is 1300 °C

Рис. 7. Зависимости в координатах уравнения Гинстлинга-Броунштейна для смесей: П+К (1); П+К(ПМ) (2); П(ПМ)+К (3); (П+К)(ПМ) (4); (П+К)(ШКМ) (5); (П+ГК)(ПМ) (6); (П+Г00)(ПМ) (7); (П+РГ)(ПМ) (8); ПГК+П (9). Температура обжига 1300 °C

Table 2

Effective rate constants of $MgAl_2O_4$ formation (1300 °C)

***Таблица 2.* Эффективные константы скорости реакции образования $MgAl_2O_4$ (1300 °C)**

Reaction mixture designation	Rate constants $K \cdot 10^6$, s^{-1}
P+C	1.7 ± 0.1
P+C(PM)	4.1 ± 0.2
P(PM)+C	8.3 ± 0.2
(P+C)(PM)	10.1 ± 0.5
(P+C)(BRM)	2.9 ± 0.2
(P+GC)(PM)	10.2±0.8
(P+G-00)(PM)	10.5±0.4
(P+RG)(PM)	10.8±0.5
XCP+P	7.3±0.2

The obtained constant values indicate a greater efficiency of impact processing. Co-mechanical activation of reagents in a planetary mill can increase the reaction rate by ~ 5 times, while abrasion in a ball-ring mill is only 1.7 times. Pretreatment of one component of the charge in PM is the most expedient for periclase, since it allows accelerating the reaction by ~ 5 times, and is also energetically and technologically the most rational due to the treatment of only one component of reduced hardness [25]. The use of xerogel combustion product in the synthesis of spinel is very effective, because it accelerates the process by ~4 times even without preliminary activation by mechanical means.

CONCLUSION

A comparison of the efficiency of solid-phase synthesis of magnesia spinel $MgAl_2O_4$ from magnesia and alumina using a mechanical activation of initial reagents and industrial powders (corundum powder KP, alumina: metallurgical GK, non-metallurgical G-00, reactive RG) and xerogel combustion product from aluminum nitrate and citric acid as a source of Al_2O_3 was carried out. It is shown that in the presence of the combustion product, the spinel yield increases significantly, approaching the synthesis productivity after preliminary mechanical treatment of the reaction mixture containing one of the industrial alumina powders.

ACKNOWLEDGEMENTS

The work was carried out within the framework of the state assignment for the implementation of research work (Topic No. FZZW-2024-0004). The study was carried out using the resources of the Center for Collective Use of Scientific Equipment of ISUCT (with the support of the Ministry of Education and Science of the Russian Federation, agreement No. 075-15-2021-671).

The authors declare the absence a conflict of interest warranting disclosure in this article.

Работа выполнена в рамках государственного задания на выполнение НИР (Тема № FZZW-2024-0004). Исследование выполнено с использованием ресурсов Центра коллективного пользования научной аппаратурой ИГХТУ (при поддержке Минобрнауки России, № 075-15-2021-671).

Авторы заявляют об отсутствии конфликта интересов, требующего раскрытия в данной статье.

REFERENCES
ЛИТЕРАТУРА

1. **Obradović N., Filipović S, Fahrenholtz W.G., Marinkovic B.A., Rogan J., Lević S., Đorđević A., Pavlović V.B.** Morphological and structural characterization of $MgAl_2O_4$ spinel. *Sci. Sinter*. 2023. V. 55. N 1. P. 1-10. DOI: 10.2298/SOS2301001O.
2. **Chen Z., Yan W., Li G., Hong S., Li N.** Enhanced mechanical properties of novel Al_2O_3-based ceramic filter by using microporous corundum-spinel and nano-Al_2O_3 powders. *J. Eur. Ceram. Soc.* 2024. V. 44. N 2. P. 1070-1080. DOI: 10.1016/j.jeurceramsoc.2023.10.004.
3. **Gajdowski C., D'Elia R., Faderl N., Bohmler J., Lorgouilloux Y., Lemonnier S., Leriche A.** Mechanical and optical properties of $MgAl_2O_4$ ceramics and ballistic efficiency of spinel based armour. *Ceram. Int.* 2022. V. 48. N 13. P. 18199−18211. DOI: 10.1016/j.ceramint.2022.03.079.
4. **Baruah B., Bhattacharyya S., Sarkar R.** Synthesis of magnesium aluminate spinel – An overview. *Appl. Ceram. Technol.* 2023. V. 20. N. 3. P. 1331-1349. DOI: 10.1111/ijac.14309.
5. **Egorov S.V., BykovY.V., Eremeev A.G., Sorokin A.A., Serov E.A., Parshin V.V., Balabanov S.S., Belyaev A.V., Novikova A.V., Permin D.A.** Milimiter-wavelength radiation used to sinter radiotransparent $MgAl_2O_4$ ceramics. *Radiophys. Quantum Electron*. 2017. V. 59. P. 690–697. DOI: 10.1007/s11141-017-9736-8.
6. **Fu L., Gu H., Huang A., Zhang M., Hong X., JinL.** Possible improvements of alumina–magnesia castable by lightweight microporous aggregates. *Ceram. Int.* 2015. V. 41. P. 1263-1270. DOI: 10.1016/j.ceramint.2014.09.056.
7. **Shahbazi H., Shokrollahi H., Alhaji A.** Optimizing the gel-casting parameters in synthesis of $MgAl_2O_4$ spinel. *J. Alloys Compd.* 2017. V. 712. P. 732-741. DOI: 10.1016/j.jallcom.2017.04.042.
8. **Zegadi A., Kolli M., Hamidouche M., Fantozzi G.** Transparent $MgAl_2O_4$ spinel fabricated by spark plasma sintering from commercial powders. *Ceram. Int.* 2018. V. 44. P. 18828–18835. DOI:10.1016/j.ceramint.2018.07.117.
9. **Peng W., Chen Z., Yan W., Schafföner S., Li G., Li Y., Jia C.** Advanced lightweight periclase-magnesium aluminate spinel refractories with high mechanical properties and high corrosion resistance. *Construct. Build. Mater.* 2021. V. 291. P. 123388. DOI: 10.1016/j.conbuildmat.2021.123388.
10. **Obradović N., Fahrenholtz W.G., Filipović S., Corlett C., Đorđević P., Rogan J., VulićP. J., Buljak V., Pavlović V.** Characterization of $MgAl_2O_4$ sintered ceramics. *Sci. Sinter*. 2019. V. 51. N 4. P. 363–376. DOI: 10.2298/SOS1904363O.
11. **Zhou Y., Ye. D., Wu Y., Zhang Ch., Bai W., Tian Y., Qin M.** Low-cost preparation and characterization of $MgAl_2O_4$ ceramics. *Ceram. Int.* 2022. V. 48.N. 5. P. 7316−7319. DOI: 10.1016/j.ceramint.2021.11.196.
12. **Klaus S., Buhr A., Bauer M., Göbbels M., Dutton J.** Formation of hexa-aluminate solid solution phases in spinel containing castables – Mineralogical investigations in the system CaO-Al_2O_3-MgO. 62nd International Colloquium on Refractories 2019 – Supplier Industries enabling REFRACTORIES. Aachen, Germany 25-26 September. 2019. P. 90-94.
13. **Kaur P., Rani S.** Effect of sintering temperature on structural and optical properties of magnesium aluminate spinel. *J. Optics.* 2023. V. 52. N 4. P. 2366-2374. DOI: 10.1007/s12596-023-01167-0.
14. **Suresh M.B., Biswas P., Saha B.P., Johnson R.** Fabrication of optically transparent $MgAl_2O_4$ polycrystalline ceramics and evaluation of high temperature dielectric, impedance spectroscopy & AC conductivity. *J. Mater. Sci. Mater. Electron.* 2023. V. 34. N 27. DOI: 10.1007/s10854-023-11315-8.
15. **Feldbach E., Kudryavtseva I., Mizohata K., Prieditis G., Räisänen J., Shablonin E., Lushchik A.** Optical characteristics of virgin and proton-irradiated ceramics of magnesium aluminate spinel. *Opt. Mater.* 2019. V. 96. 109308. DOI:10.1016/j.optmat.2019.109308.
16. **Talimian A., Pouchly V., El-Maghraby H. F., Maca K., Galusek D.** Transparent magnesium aluminate spinel: Effect of critical temperature in two-stage spark plasma sintering. *J. Eur. Ceram. Soc.* 2020. V. 40. N 6. P. 2417–2425. DOI: 10.1016/j.jeurceramsoc.2020.02.012.
17. **Salem S., Nouri B., Ghadiri M.** Photoactivity of magnesium aluminate under solar irradiation for treatment of wastewater contaminated by methylene blue: Effect of self-combustion factors on spinel characteristics. *Solar Energy Mater. Solar Cells.* 2020. V. 218. P. 110773. DOI: 10.1016/j.solmat.2020.110773.
18. **Asl E. A., Haghighi M., Talati A.** Enhanced simulated sunlight-driven magnetic $MgAl_2O_4$-AC nanophotocatalyst for efficient degradation of organic dyes. *Separat. Purificat. Technol.* 2020. V. 251. P. 117003. DOI: 10.1016/j.seppur.2020.117003.

19. **Prieditis G., Feldbach E., Kudryavtseva I., Popov A. I., Shablonin E., Lushchik A.** Luminescence characteristics of magnesium aluminate spinel crystals of different stoichiometry. *IOP Conf. Ser.: Mater. Sci. Eng.* 2019. V. 503. P. 012021. DOI: 10.1088/1757-899x/503/1/012021.
20. **Klym H., Ingram A., Shpotyuk O., Hadzaman I., Hotra O., Kostiv Yu.** Nanostructural free-volume effects in humidity-sensitive MgO–Al_2O_3 ceramics for sensor applications. *J. Mater. Eng. Perform.* 2016. V. 25. P. 866–873. DOI: 10.1007/s11665-016-1931-9.
21. **Habibi N., Wang Y., Arandiyan H., Rezaei M.** Effect of substitution by Ni in $MgAl_2O_4$ spinel for biogas dry reforming. *Int. J. Hydrog. Energy.* 2017. V. 42. N 38. P. 24159–24168. DOI: 10.1016/j.ijhydene.2017.07.222.
22. **Tang C., Zhai Z., Li X., Sun L., Bai W.** Sustainable production of acetaldehyde from lactic acid over the magnesium aluminate spinel. *J. Taiwan Inst. Chem. Eng.* 2015. V. 58. P. 97-106. DOI: 10.1016/j.jtice.2015.06.014.
23. **Singh A.K., Sarkar R.** Development of spinel sol bonded high pure alumina castable composition. *Ceram. Int.* 2016. V. 42. N 15. P. 17410–17419. DOI: 10.1016/j.ceramint.2016.08.041.
24. **Ikonnikova O.P., Popova N.A.** Silicon carbide ceramics bonded with alumina-magnesia spinel. *Usp. Khim. Khim. Tekhnol.* 2018. V. XXXII. N 2. P. 83-85 (in Russian). **Иконникова О.П., Попова Н.А.** Керамика из карбида кремния на связке из алюмомагнезиальной шпинели. *Усп. в химии и хим. технологии.* 2018. Т. XXXII. № 2. С. 83-85.
25. **Kosenko N.F., Smirnova M.A.** Synthesis of magnesia-aluminate spinel from oxides with different histories. *Ogneupory Tekhnich. Keram.* 2011. N 9. P. 3-11 (in Russian). **Косенко Н.Ф., Смирнова М.А.** Синтез магнезиальноалюминатной шпинели из оксидов с различной предысторией. *Огнеупоры и техническая керамика*. 2011. N 9. С. 3-11.
26. **Kafili G., Alhaji A.** The effects of different precipitant agents on the formation of alumina-magnesia composite powders as the magnesium aluminate spinel precursor. *Adv. Powder Technol.* 2019. V. 30. P. 1108-1115. DOI: 10.1016/j.apt.2019.03.007.
27. **Nam S., Lee M., Kim B.-N., Lee Y., Kang S.** Morphology controlled Co-precipitation method for nano structured transparent $MgAl_2O_4$. *Ceram. Int.* 2017. V. 43. N 17. P. 15352–1535. DOI: 10.1016/j.ceramint.2017.08.075.
28. **Zhurba E.V., Lemeshev D.O., Popova N.A.** Precursor of alumina-magnesia spinel obtained by reverse heterophase co-precipitation for transparent ceramics. *Usp. Khim. Khim. Tekhnol.* 2016. V. XXX. N 7. P. 39-40 (in Russian). **Журба Е.В., Лемешев Д.О., Попова Н.А.** Прекурсор алюмомагнезиальной шпинели, полученной методом обратного гетерофазного соосаждения для прозрачной керамики. *Усп. в химии и хим. технологии.* 2016. Т. XXX. № 7. С. 39-40.
29. **Viswanathan T., Pal S., Rahaman A.** Synthesis of magnesium aluminate spinel nanocrystallites by co-precipitation as function of pH and temperature. *Sādhanā*. 2020. V. 45. P. 17. DOI: 10.1007/s12046-020-1265-z.
30. **Sanjabi S., Obeydavi A.** Synthesis and characterization of nanocrystalline $MgAl_2O_4$ spinel via modified sol–gel method. *J. Alloys Compd.* 2015. V. 645. P. 535-540. DOI: 10.1016/j.jallcom.2015.05.107.
31. **Wen Y., Liu X., Chen X., Jia Q., Yu R., Ma T.** Effect of heat treatment conditions on the growth of $MgAl_2O_4$ nanoparticles obtained by sol-gel method. *Ceram. Int.* 2017. V. 43. P. 15246-15253. DOI: 10.1016/j.ceramint.2017.08.061.
32. **Edrees S.J., Kareem S.J., Fadel A.M.** Morphological characterzations of spinel nanoparticles synthesized by sol-gel method. *J. Phys. Conf. Ser.* 2021. V. 1973. P. 012132. DOI: 10.1088/1742-6596/1973/1/012132.
33. **Habibi N., Wang Y., Arandiyan H., Rezaei M.** Low-temperature synthesis of mesoporous nanocrystalline magnesium aluminate ($MgAl_2O_4$) spinel with high surface area using a novel modified sol-gel method. *Adv. Powder Technol.* 2017. V. 28. P. 1249–1257. DOI: 10.1016/j.apt.2017.02.012.
34. **Khomidov F., Kadyrova Z., Usmanov K.L., Niyazova S.M., Sabirov B.** Peculiarities of sol-gel synthesis of aluminum-magnesium spinel. *Glass Ceram.* 2021. V. 78. P. 251–254. DOI: 10.1007/s10717-021-00389-7.
35. **Jiang F., Feng G., Xu C., Qing S., Wu Q., Yu Y., Zhang Q., Jiang W.** Novel facile nonhydrolytic sol-gel synthesis of $MgAl_2O_4$ nanocrystal from bimetallic alkoxides. *J. Sol−Gel Sci. Technol.* 2021. N 100. P. 555−561. DOI: 10.1007/s10971-021-05663-2.
36. **Valente J. S., Rodriguez-Gattorno G., Valle-Orta M., Torres-Garsia E.** Thermal decomposition kinetics of MgAl layered double hydroxides. *Mater. Chem. Phys*. 2012. V. 133. P. 621-629. DOI: 10.1016/j.matchemphys.2012.01.026.
37. **Rahmat N., Yaakob Z., Pudukudy M., Rahman N.A., Jahaya S.S.** Single step solid-state fusion for MgAl2O4 spinel synthesis and its influence on the structural and textural properties. *Powder Technol.* 2018. V. 329. P. 409-419. DOI: 10.1016/j.powtec.2018.02.007.
38. **Vahid B.R., Haghighi M., Toghiani J., Alaei S.** Hybrid co-precipitation vs. combustion synthesis of Mg-Al spinel based nanocatalyst for efficient biodiesel production. *Energy Convers. Manag.* 2018. V. 160. P. 220-229. DOI: 10.1016/j.enconman.2018.01.030.
39. **Radishevskaya N.I., Lepakova O.K., Nazarova A.Yu., Kitler V.D., Gabbasov R.M., Minin R.V.** Characteristics of phase formation during combustion of the MgO-Al_2O_3-$Mg(NO_3)_2 \cdot 6H_2O$-Al-B system. *Ceram. Int.* 2022. V. 48. N 10. P. 13948-13959. DOI: 10.1016/j.ceramint.2022.01.279.
40. **Nassar M.Y., Ahmed I. S., Samir I.** A novel synthetic route for magnesium aluminate (MgAl2O4) nanoparticles using sol-gel auto combustion method and their photocatalytic properties. *Spectrochim. Acta A Mol. Biomol. Spectrosc.* 2014. V. 131. P. 329–334. DOI: 10.1016/j.saa.2014.04.040.
41. **Ganesh I., Srinivas B., Johnson R., Saha B.P., Mahajan Y.R.** Effect of fuel type on morphology and reactivity of combustion synthesised $MgAl_2O_4$ powders. *Br. Ceram. Trans.* 2002. V. 101. N 6. P. 247-254. DOI: 10.1179/096797802225004063.
42. **Mukherjee S., Ghosh S.R., Banerjee S.** Evolution of Magnesium Aluminate Spinel by Combustion route and its characterization. 2020 IEEE 1st International Conference for Convergence in Engineering (ICCE). Kolkata. India. 2020. P. 65-67. DOI: 10.1109/ICCE50343.2020.9290571.
43. **Balalizadeh H., Abbasian A.R., Afarani M.Sh.** Preparation of pure cordierite through heat treatment of combustion synthesized magnesium aluminate spinel and silica nanoparticles. *J. Part. Sci. Technol.* 2023. V. 9. N 1. P. 11-18. DOI: 10.22104/jpst.2023.6295.1229.
44. **Özdemiř H., Öksüzomer M.A.F.** Synthesis of Al_2O_3, MgO and $MgAl_2O_4$ by solution combustion method and investigation of performances in partial oxidation of methane. *Powder Technol.* 2020. V. 359. P. 107−117. DOI: 10.1016/j.powtec.2019.10.001.
45. **Radishevskaya N.I., Nazarova A.Yu., L'vov O.V., Kasatskii N.G., Salamatov V.G., Saikov I.V., Kovalev D.Yu.** Self-propagating high-temperature synthesis of $MgAl_2O_4$ spinel. *Inorg. Mater.* 2020. V. 56. N 2. P. 142-150. DOI: 10.1134/S0020168520010112.

46. **Wang Y., Xie X., Zhu C.** Self-propagating high-temperature synthesis of magnesium aluminate spinel using Mg−Al alloy. *ACS Omega.* 2022. V. 7. P. 12617−12623. DOI: 10.1021/acsomega.1c06583.
47. **Tran A., TranV., Nguyet N.T.M., Luong A.T., Le T.V., Phuc N.H.H.** Solid-State Reaction Synthesis of $MgAl_2O_4$ Spinel from MgO–Al_2O_3 Composite Particles Prepared via Electrostatic Adsorption. *ACS Omega.* 2023. V. 8. P. 36253−36260. DOI: 10.1021/acsomega.3c04782.
48. **Sun X., Jiang X., Shan Y., Han X., Xu J., Li J.** Low temperature solid reaction synthesis of high sinter ability $MgAl_2O_4$ powder from γ-Al_2O_3+MgO and θ/α-Al_2O_3+MgO batches. *Ceram. Int.* 2022. V. 48. P. 17471−17480. DOI: 10.1016/j.ceramint.2022.03.011.
49. **Sarkar R., Sahoo S.** Effect of raw materials on formation and densification of magnesium aluminate spinel. *Ceram. Int.* 2014. V. 40. P. 16719–16725. DOI: 10.1016/j.ceramint.2014.08.037.
50. **Gumennikova E.A., Titov D.D., Lysenkov A.S., Frolova M.G., Kargin Yu.F., Shcherbakova G.I. Novokovskaya E.A.** Rheological properties of MgAl2O4 obtained from preceramic organomagnesiumoxanealumoxanes. *J. Phys.: Conf. Ser*. 2019. V. 1347. N 1. P. 012062. DOI: 10.1088/1742-6596/1347/1/012062.
51. **Yan W., Lin X.L., Chen J.F., Li N., Wei Y.W., Han B.Q.** Effect of TiO_2 addition on microstructure and strength of porous spinel ($MgAl_2O_4$) ceramics prepared from magnesite and $Al(OH)_3$. *J. Alloys Compd.* 2015. V. 618. P. 287-291. DOI: 10.1016/j.jallcom.2014.08.169.
52. **Miroliaee A., Salehirad A., Rezvani A.R.** Synthesis of high-surface-area spinel-type $MgAl_2O_4$ nanoparticles by $[Al(sal)_2(H_2O)_2]_2$ $[Mg(dipic)_2]$ and $[Mg(H_2O)_6][Al(ox)_2(H_2O)_2]_2 \cdot 5H_2O$: influence of inorganic precursor type. *Bull. Mater. Sci.* 2017. V. 40. P. 45–53. DOI: 10.1007/s12034-016-1353-1.
53. **Macaigne R., Marinel S., Goeuriot D., Saunier S.** Sintering paths and mechanisms of pure $MgAl_2O_4$ conventionally and microwave sintered. *Ceram. Int.* 2018. V. 44. P. 21107–21113. DOI: 10.1016/j.ceramint.2018.08.149.
54. **Li R., Liu J.** Effect of reaction time on the synthesis and sintering of magnesium-aluminium spinel by microwave hydrothermal synthesis. *Transact. Indian Ceram. Soc.* 2021. V. 80. N 4. P. 265-269. DOI: 10.1080/0371750X.2021.2014637.
55. **Косенко Н.Ф., Филатова Н.В., Егорова А.А.** Синтез магнезиохромита ($MgCr_2O_4$): влияние предварительной механической и микроволновой обработки прекурсоров. *Изв. вузов. Химия и хим. технология.* 2020. Т. 63. Вып. 8. С.96-102. **Kosenko N.F., Filatova N.V., Egorova A.A.** Magnesiochromite ($MgCr_2O_4$) synthesis: effect of mechanical and microwave pretreatment. *ChemChemTech [Izv. Vyssh. Uchebn. Zaved. Khim. Khim. Tekhnol.]*. 2020. V. 63. N 8. P. 96-102. DOI: 10.6060/ivkkt.20206308.6214.
56. **Abdi M. S., Ebadzadeh T., Ghaffari A., Feli M.** Synthesis of nano-sized spinel (MgAl2O4) from short mechanochemically activated chloride precursors and its sintering behavior. *Adv. Powder Technol.* 2015. V. 26. P. 175-179. DOI: 10.1016/j.apt.2014.09.011.
57. **Tavangarian F., Li G.** Mechanical activation assisted synthesis of nanostructure $MgAl_2O_4$ from gibbsite and lansfordite. *Powder Technol*. 2014. V. 267. P. 333–338. DOI: 10.1016/j.powtec.2014.08.003.
58. **Liu J., Lv X., Li J., Zeng X., Xu Z., Zhang, Jiang L.** Influence of Parameters of high-energy ball milling on the synthesis and densification of magnesium aluminate spinel. *Sci. Sinter*. 2016. V. 48. P. 353-362. DOI: 10.2298/SOS1603353L.
59. **Obradovic N., Fahrenholtz W. G., Filipovic S., Markovic S., Blagojevic V., Levic S., Savic S., Djordjevic A., Pavlovic V.** Formation kinetics and cation inversion in mechanically activated $MgAl_2O_4$ spinel ceramics. *J. Thermal Anal. Calorim.* 2020. V. 140. P. 95–107. DOI: 10.1007/s10973-019-08846-w.
60. **Kosenko N.F., Smirnova M.A.** Evaluation of the effectiveness of mechanical processing of aluminum oxide based on thermochemical data. *ChemChemTech [Izv. Vyssh. Uchebn. Zaved. Khim. Khim. Tekhnol.]*. 2008. V. 51. N 10. P. 122-124 (in Russian). **Косенко Н.Ф., Смирнова М.А.** Оценка эффективности механической обработки оксида алюминия на основе термохимических данных. *Изв. вузов. Химия и хим. технология.* 2008. Т. 51. Вып. 10. С. 122-124.
61. **Kosenko N.F., Filatova N.V.** Regulating the sinterability of magnesium oxide using various types of mechanochemical treatment. *ChemChemTech [Izv. Vyssh. Uchebn. Zaved. Khim. Khim. Tekhnol.]*. 2009. V. 52. N 9. P. 80-84. **Косенко Н.Ф., Филатова Н.В.** Регулирование спекаемости оксида магния с помощью механохимической обработки различного типа. *Изв. вузов. Химия и хим. технология.* 2009. Т. 52. Вып. 9. С. 80-84.
62. **Филатова Н.В., Косенко Н.Ф., Баданов М.А.** Физико-химическое изучение поведения муллитового прекурсора, синтезированного соосаждением. *Изв. вузов. Химия и хим. технология.* 2021. Т. 64. Вып. 11. С. 97-102. **Filatova N.V., Kosenko N.F., Badanov M.A.** Physico-chemical study of the behavior of a mullite precursor synthesized with co-precipitation. *ChemChemTech [Izv. Vyssh. Uchebn. Zaved. Khim. Khim. Tekhnol.]*. 2021. V. 64. N 11. P. 97-102. DOI:10.6060/ivkkt.20216411.6478.

Поступила в редакцию 20.02.2024
Принята к опубликованию 03.04.2024

Received 20.02.2024
Accepted 03.04.2024